Article

pubs.acs.org/Biomac

Bioinspired Self-Assembled Peptide Nanofibers with Thermostable Multivalent α-Helices

So-hee Han, Mun-kyung Lee, and Yong-beom Lim*

Translational Research Center for Protein Function Control and Department of Materials Science and Engineering, Yonsei University, Seoul 120-749, Korea

Supporting Information

ABSTRACT: The stabilization of peptide's active conformation is a critical determinant of its target binding efficiency. Here we present a structure-based self-assembly strategy for the design of nanostructures with multiple and thermostable α-helices using bioinspired peptide amphiphiles. The design principle was inspired by the oligomerization of the human immunodeficiency virus type-1 (HIV-1) Rev protein. Our goal was to find a strategy to modify the Rev protein into a chemically manageable self-assembling peptide while stabilizing its α-helical structure. Instead of using cyclic peptides for structure stabilization, this strategy utilizes the pseudocyclization for helix stabilization. The self-assembly induced stabilization of α-helical conformation could be observed, and the α-helices were found to be stable even at high temperature (at least up to 74 °C). Conjugation of a hydrophobic alkyl chain to the Rev peptide was crucial for forming the self-assembled nanostructures, and no nanostructures could be obtained without this modification. Because chemical modifications to the α-helical peptide domain can be avoided, potentially any α-helical peptide fragment can be grafted into this self-assembling peptide scaffold.

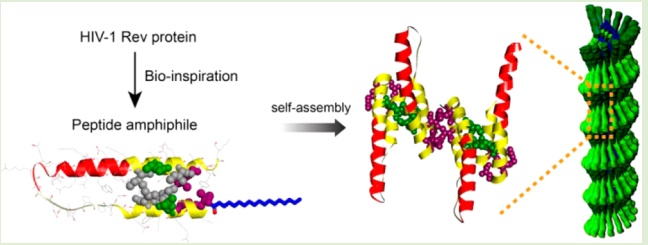

INTRODUCTION

The α-helix is one of the most crucial secondary structural motifs found in proteins. In fact, the secondary structure of typical globular proteins contains more than 30% α-helix domains.[1] Importantly, many α-helices play fundamental roles in the mediation of specific biomacromolecular interactions such as protein−protein, protein−DNA, and protein−RNA interactions. α-Helical structures can be maintained within the context of intact proteins, due to conformational constraints and a number of stabilizing interactions provided by the protein environment.[2,3] In contrast, the α-helix, when isolated from the protein as a peptide, is rarely helical and conformationally heterogeneous due to its intrinsic thermodynamic instability.

Because the stabilization of peptide's active conformation is a critical determinant of its target binding efficiency, many attempts have been made to construct stabilized α-helical structures in the form of peptides. These approaches can be classified based on the number of helices to be stabilized, that is, monomeric and multimeric approaches. In the monomeric approach, peptide α-helical structures have been stabilized by constraining the peptide backbone through the formation of chemical cross-links[3−5] or noncovalent bridge formation,[6,7] incorporating natural or unnatural amino acids with helix-favoring properties[3,8] or capping or nucleating helix formation.[9,10] These monomeric approaches often entail chemical modifications of the α-helical peptides. Multimeric approaches are in the beginning stages of development. Recently, it was shown that nanostructures with multiple stabilized α helices can be constructed by applying a peptide self-assembly approach, in which the self-assembly mediated coil-to-rod transition in the β-sheet segment of a macrocyclic peptide can constrain and thereby stabilize the α-helical segment.[11−14] When this cost-effective self-assembly approach is applied, nanostructures with multiple stabilized α-helices can be obtained, which can potentially be used in the modulation of biological multivalent interactions. Moreover, because chemical modifications to the α-helical peptide domain can be avoided, potentially any α-helical peptide fragment can be grafted into the self-assembling peptide scaffold.

In this work, we present a simple but powerful self-assembly strategy for the design of nanostructures with multiple stabilized α helices using bioinspired peptide amphiphiles. This strategy utilizes the pseudocyclization effect for helix stabilization. The design principle was inspired by the oligomerization of the human immunodeficiency virus type-1 (HIV-1) Rev protein.[15]

EXPERIMENTAL SECTION

Materials. Fmoc-amino acids and coupling reagents were purchased from Novabiochem (Germany) and Anaspec (U.S.A.). General chemicals were obtained from Sigma-Aldrich (U.S.A.) and Merck (Germany). Stearic acid was purchased from Sigma-Aldrich. High-performance liquid chromatography (HPLC) solvents were purchased from Fisher Scientific (U.S.A.). To make it quite sure that the peptide assemblies were in a thermodynamic equilibrium state, we

Received: February 12, 2013
Revised: March 20, 2013
Published: April 3, 2013

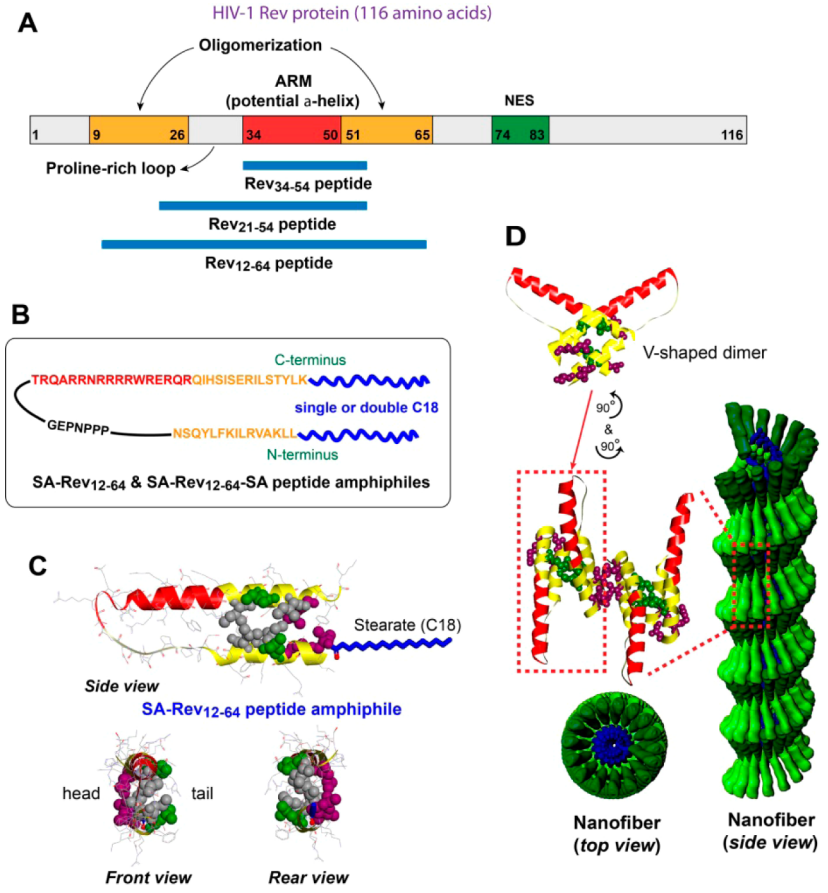

Figure 1. Self-assembling peptide amphiphiles derived from HIV-1 Rev protein. (a) The domain structure of Rev, and the Rev peptides used in this study. (b) A schematic structure of SA-Rev$_{12-64}$ and SA-Rev$_{12-64}$-SA peptide amphiphiles (a helix−loop−helix structure with single or double C18 alkyl chains; red, α-helical ARM motif; yellow, oligomerization domain; black, proline-rich loop). (c) A model of the stabilized helical hairpin structure of SA-Rev$_{12-64}$. Hydrophobic amino acids at the intramolecular interface (gray) and intermolecular oligomerization interfaces (purple, head; green, tail). (d) A model depicting the detailed molecular structure of a nanofiber formed by the self-assembly of the SA-Rev$_{12-64}$ peptide amphiphiles. The helical hairpin structures are adopted from Rev X-ray crystal structures (Protein Data Bank accession numbers, 2X7L and 3LPH). The model is tentative because it is not derived from structural data.

incubated all samples for several days before taking measurements. Repeated experiments revealed that steady state has been reached after the incubation period.

Peptide Amphiphile Synthesis. Standard amino acid protecting groups were employed for the synthesis. The Rev$_{34-54}$ peptide and Rev$_{21-54}$ peptide were synthesized on 2-Chlorotrityl resin preloaded with Fmoc-Ser-OH. Further couplings of amino acids were performed on a Tribute peptide synthesizer on 0.1 mmol scale (Protein Technologies). The Rev$_{12-64}$ peptide, SA-Rev$_{12-64}$ peptide amphiphile, and SA-Rev$_{12-64}$-SA peptide amphiphile were synthesized on a Rink Amide MBHA resin LL (Novabiochem). The Rev$_{12-64}$ peptide, SA-Rev$_{12-64}$ peptide amphiphile, SA-Rev$_{12-64}$-SA peptide amphiphile contain Lys(Mmt) residue at C-terminus for orthogonal deprotection. For the synthesis of the SA-Rev$_{12-64}$-SA peptide amphiphile, the Mmt group in Lys side chain was orthogonally deprotected using methylene chloride (MC)/2,2,2-trifluoroethanol (TFE)/AcOH (6:2:2). Then, stearic acid was coupled to the N-terminal α-amine and the ε-amine group of lysine residue using *O*-(benzotriazol-1-yl)-*N*,*N*,*N*′,*N*′-tetramethyluronium hexafluorophosphate (HBTU) and *N*,*N*-diisopropylethylamine (DIPEA). For SA-Rev$_{12-64}$ peptide amphiphile synthesis, N-terminal α-amine group was conjugated with stearic acid. For final deprotection and cleavage from the resin, resin-bound peptide was treated with a cleavage cocktail [trifluoroacetic acid (TFA)/triisopropylsilane (TIS)/water] (95:2.5:2.5) for 3 h, and was triturated with *tert*-butyl methyl ether. The peptides were purified by reverse-phase HPLC (water−acetonitrile with 0.1% TFA). The molecular weight was confirmed by matrix-assisted laser desorption/ionization time-of-flight (MALDI-TOF) mass spectrometry. Concentration was determined spectrophotometrically in water/acetonitrile (1:1) using a molar extinction coefficient of tryptophan (5690 M^{-1} cm^{-1}) and tyrosine (1280 M^{-1} cm^{-1}) at 280 nm.

CD Spectroscopy. Circular dichroism (CD) spectra were measured using a Chirascan CD spectrometer equipped with peltier temperature controller (Applied Photophysics). Spectra were recorded from 260 to 190 nm using the 2 or 10 mm path-length cuvettes. Scans were repeated five times and averaged. Molar ellipticity was calculated per amino acid residue. Peptide concentration was typically 15 μM unless noted otherwise.

Fluorescence Polarization Spectroscopy. Fluorescence polarization spectrum was acquired using a Chirascan spectrometer equipped with FP.3 fluorescence polarization accessory (Applied Photophysics). The spectrometer was calibrated using a sample with a known anisotropy. We typically used Rose Bengal. Spectra were recorded from 300 to 280 nm in 10 mm path-length cuvettes using a 320 nm cutoff filter. Scans were repeated five times and averaged.

Solubility Measurement. Solubility of SA-Rev$_{12-64}$ peptide amphiphile was determined at various salt concentrations. The samples (15 μM) were dissolved in 0−150 mM KF, sonicated, and incubated overnight. Then samples was centrifuged at the maximum speed of tabletop centrifuge (RCF: 16110 × g) for 5 min, and the supernatants were collected. Absorbance was measured using a NanoDrop spectrophotometer (Thermo Scientific). The measurements were repeated three times and averaged.

dx.doi.org/10.1021/bm400233x | *Biomacromolecules* 2013, 14, 1594−1599

Transmission Electron Microscopy. A 10 μL aliquot of sample (typically, 1−100 μM) was placed onto a carbon-coated copper grid and incubated for 1 min. The sample was then wicked off by filter paper. The sample was stained with 1% uranyl acetate for negative staining. The specimens were observed using a JEOL-JEM 2010 instrument operating at 120 kV. The data were analyzed using DigitalMicrograph software.

Atomic Force Microscopy. For atomic force microscopy (AFM), typically 5 μL of the sample was deposited onto a freshly cleaved mica surface for 1 min. Then, the sample was wicked off by filter paper and dried. The images were obtained in tapping mode with a Nanoscope IV instrument (Digital Instruments). AFM scans were taken at a set point of 1.2−1.5 V and a scanning speed was 0.5 Hz.

RESULTS AND DISCUSSION

Rev is an essential viral protein responsible for the nucleocytoplasmic export of viral RNA.[15] Rev binds to the Rev response element (RRE), which is an approximately 350-nt structured RNA within the viral mRNA. Rev initially binds to the high-affinity site (stem-loop IIB) within the RRE using a 17-amino acid α-helical arginine-rich motif (ARM; Figure 1).[16] After initial binding, 7−9 additional molecules of Rev cooperatively oligomerize along the various low-affinity sites in the RRE.[17−19] By interacting with the nuclear export factor CRM1/exportin 1 via the nuclear export signal (NES) domain, these multimeric Rev assemblies mediate the export of unspliced and partially spliced HIV-1 mRNAs to the cytoplasm.[17] Recent crystallographic studies have shown that Rev adopts an antiparallel helix−loop−helix structure (here, termed a helical hairpin) within the multimeric assemblies. The helical hairpin is stabilized by a set of protein−protein and protein−RNA interactions (Figure 1c).[18,19] Helix stabilization and oligomerization are largely driven by hydrophobic interactions between several hydrophobic amino acids within the oligomerization domain (Figure 1c).

Based on these previous findings and structural data, our goal was to find a strategy to modify the Rev protein into a chemically manageable peptide while stabilizing its α-helical structure. It has been reported that the helical stability of the Rev ARM (a.a. 34−50) correlates well with its specific binding to the RNA.[20] We first examined the helical stability of several Rev-derived peptides. The Rev_{34-54} peptide is a 21-amino acid peptide consisting of a Rev ARM and a truncated C-terminal oligomerization domain (only approximately 1/4 of the oligomerization domain remains). Investigation of the peptide secondary structure by circular dichroism (CD) spectroscopy revealed that the Rev_{34-54} peptide exists almost in a random coil conformation (Figure 2a).

The 34-mer Rev_{21-54} peptide contains truncated N- and C-terminal fragments of oligomerization domains. This peptide was also almost in a random coil state in pure water (Figure 2b). However, an increase in helical content was evident when the Rev_{21-54} peptide was dissolved in phosphate-buffered saline (PBS; 15 mM potassium phosphate, 150 mM potassium fluoride, pH 7.4), as evidenced by both the appearance of a distinct band at 222 nm, which is a signature of α-helix, and an increase in the $[\theta]_{222}/[\theta]_{208}$ ratio from 0.28 (pure water) to 0.48 (PBS). Potassium fluoride (KF) was used because it is typically preferred over NaCl for increasing the ionic strength during CD measurements, as the chloride ion has a strong UV absorbance at low wavelengths. The $[\theta]_{222}/[\theta]_{208}$ ratio is sensitive to the backbone dihedral angles and can be used as a measure of α-helicity, increasing as the helicity increases.[21] The Rev_{21-54} peptide contains Leu-22 and Ile-52, a pair of amino acids that form hydrophobic cluster at the intramolecular interface (Figures 1c and S3). The increased ion strength in PBS is likely responsible for the increased helicity because hydrophobic interactions strengthen with increasing ionic strength.[22,23]

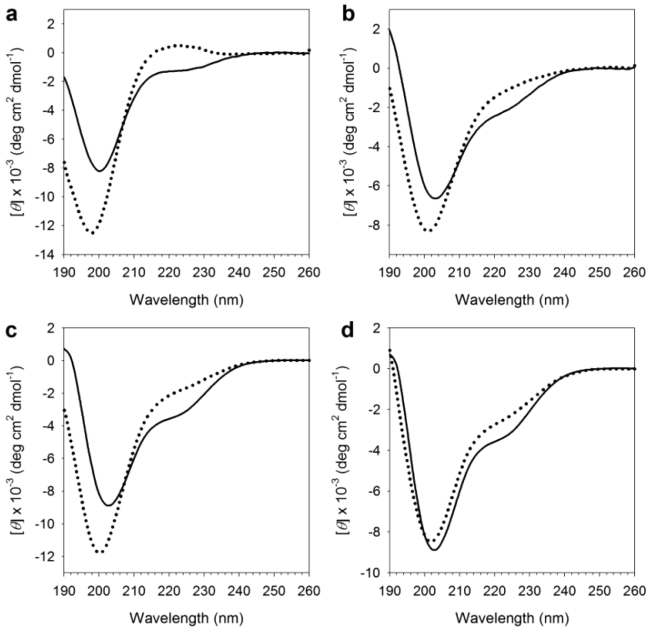

Figure 2. Investigation of the secondary structures of Rev-derived peptides using CD spectroscopy. (a) Rev_{34-54} peptide (21-mer) in water (dotted line) and PBS (solid line) at 4 °C. (b) Rev_{21-54} peptide (34-mer) in water (dotted line) and PBS (solid line) at 4 °C. (c) Rev_{12-64} peptide (54-mer) in water (dotted line) and PBS (solid line) at 4 °C. (d) Rev_{12-64} peptide (54-mer) in PBS at 25 °C (dotted line) and at 4 °C (solid line).

We subsequently synthesized a 54-mer peptide Rev_{12-64}, which spans most of both N- and C-terminal oligomerization domains. An additional Lys was introduced at the C-terminus for chemical modification (vide infra). All of the critical amino acids responsible for stabilizing the intramolecular and intermolecular hydrophobic interfaces are included in this peptide. These amino acids are Leu-18 and Ile-55 (tail intermolecular hydrophobic surface); Leu-12, Val-16, and Leu-60 (head intermolecular hydrophobic surface); Ile-19, Leu-22, Ile-52, and Ile-59 (intramolecular hydrophobic interface; Figures 1c and S4).[17]

Despite the presence of multiple hydrophobic amino acids for structural stabilization, the Rev_{12-64} peptide was found to be almost in a random coil conformation in pure water, similar to that of the two other shorter peptides (Figure 2c). The helicity also increased in PBS solution similar to the Rev_{21-54} peptide ($[\theta]_{222}/[\theta]_{208}$ ratio: pure water, 0.28, to PBS, 0.48); however, the level of stabilization was not significant and the $[\theta]_{222}/[\theta]_{208}$ ratio was similar to that of the Rev_{21-54} peptide. Helix formation is an enthalpy-driven process in which unfolding increases with temperature.[24] Therefore, the helicity of a peptide usually decreases as the temperature is increased. Accordingly, the level of helicity for the Rev_{12-64} peptide decreased at an elevated temperature, 25 °C (Figure 2d). Therefore, although the Rev_{12-64} peptide contains most of the important residues for helical hairpin stabilization, it exists largely in an unstructured form when other stabilizing interactions, such as protein−RNA interactions, are absent. In

consideration of the normal human body temperature, 37 °C, more stable structures should be developed for biological applications of multiple α-helix-stabilized nanostructures.

One of the most simple but powerful ways to create self-assembled peptide nanostructures is to conjugate hydrophobic alkyl chains to a hydrophilic peptide.[25−28] The resulting amphiphilic molecules are usually termed peptide amphiphiles (PAs). We envisioned that the conjugation of hydrophobic alkyl chains at the N- and/or C-terminus of Rev helical hairpin would strengthen the hydrophobic interactions. Thus, both the self-assembled nanostructures and the helical hairpins might be simultaneously stabilized upon conjugate aggregation. Based on this idea, we synthesized PAs with conjugated stearic acid (SA, C18:0) at the N-terminus (SA-Rev$_{12-64}$ PA) and at both of the N- and C-termini (SA-Rev$_{12-64}$-SA PA). Conjugation of SA at the C-terminus was achieved using an acid-labile methoxytrityl (Mmt) as a protective group of the C-terminal Lys side chain. The SA-Rev$_{12-64}$ PA was clearly soluble in water. In contrast, the SA-Rev$_{12-64}$-SA PA was barely soluble in water possibly due to the excessively increased hydrophobicity. Therefore, further investigations were conducted only with SA-Rev$_{12-64}$ PA.

Indeed, in comparison to the Rev$_{12-64}$ peptide, increased stabilization of the SA-Rev$_{12-64}$ PA's helical conformation was evident, as manifested by an overall red-shifted CD spectrum and an increase in the $[\theta]_{222}/[\theta]_{208}$ ratio (Figure 3a). Next, we investigated the concentration dependence of the SA-Rev$_{12-64}$ PA aggregation by acquiring fluorescence polarization (FP) spectra. We employed this method because fluorescence-based spectroscopy has a wider dynamic range over broad concentrations than CD spectroscopy. We first checked the conformation of the SA-Rev$_{12-64}$ PA in 50% 2,2,2-trifluoroethanol (TFE), which is a well-known cosolvent that helps stabilize the α-helical structures in proteins and peptides.[29] As expected, a significant level of helix stabilization was observed in the TFE solution ($[\theta]_{222}/[\theta]_{208}$ ratio = 0.76, Figure 3b).

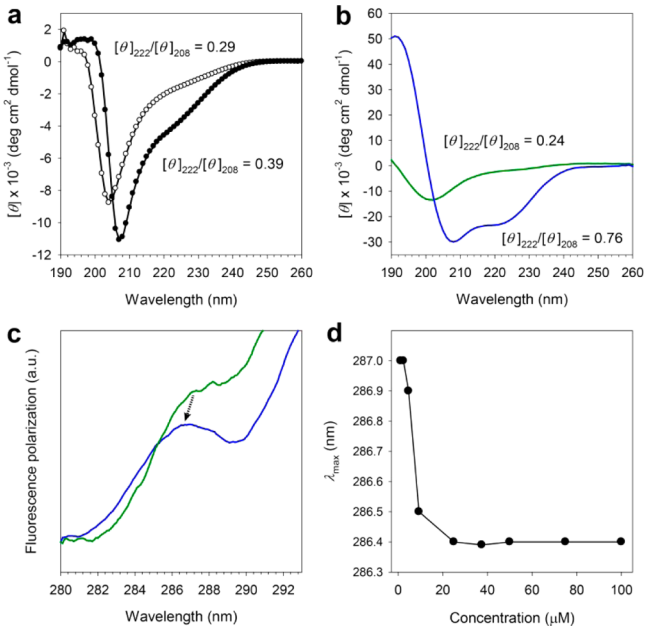

Figure 3. Self-assembly behaviors of the SA-Rev$_{12-64}$ peptide. (a) CD spectra of the Rev$_{12-64}$ peptide (open circle) and the SA-Rev$_{12-64}$ PA (closed circle). [peptide] = 100 μM in water. (b) CD spectra of the SA-Rev$_{12-64}$ PA in water (green) and 50% TFE (blue). [peptide] = 0.6 μM. (c) Normalized fluorescence polarization (FP) spectra (0.6 μM) of the SA-Rev$_{12-64}$ PA in water (green) and 50% TFE (blue). (d) Plot of the peak excitation wavelength (λ_{max}) in the FP spectra (data point interval = 0.1 nm) as a function of SA-Rev$_{12-64}$ PA concentration (in water). All of the measurements were performed at 25 °C. The wavelength of the first positive band that appears around 286−287 nm of the FP spectrum was used to plot this graph.

The same PA samples were then subjected to FP spectrum measurements. As shown in Figure 3c, a positive band with a peak excitation wavelength (λ_{max}) at approximately 286−287 nm was observed in the FP spectra. It has been shown that this band is sensitive to molecular Brownian motion and arises when tryptophan is incorporated in the α-helix.[30] We found that this band became sharper and that λ_{max} was blue-shifted from 287 to 286.4 nm when the solvent was changed from pure water to 50% TFE (Figure 3c). Therefore, the position of λ_{max} can be used as a measure of helix stability. Plotting λ_{max} as a function of the SA-Rev$_{12-64}$ PA concentration revealed that λ_{max} initially decreased in a gradual manner as the peptide concentration increased and then suddenly stopped decreasing, forming a plateau (Figures 3d and S5). These results suggest that λ_{max} decreases because molecular Brownian motion becomes restricted as the helix stabilizes. Additionally, the presence of a discontinuous change in λ_{max} likely reflects the onset of aggregation when the concentration of the amphiphile reaches a certain point. Moreover, there was a discontinuous change in peak intensity at λ_{max}, which is also likely to represent the onset of aggregation. Therefore, these results indicate the self-assembly induced stabilization of α-helical conformation.

We next examined the effect of ionic strength on SA-Rev$_{12-64}$ PA assembly. The SA-Rev$_{12-64}$ PA, although soluble in pure water, showed the formation of a precipitate in PBS solution. Hence, we first determined the solubility of the peptide. The SA-Rev$_{12-64}$ PA showed a gradual decrease in solubility as the ionic strength was increased (Figure S6). Because the peptide was quite soluble at a KF concentration of approximately 60 mM, further investigations were performed at this ionic strength. Remarkably, the α-helical structure of the SA-Rev$_{12-64}$ PA was found to be significantly stabilized in 60 mM KF solution, showing increased negative minimum of ellipticity around 208 and 222 nm (Figure 4a). The $[\theta]_{222}/[\theta]_{208}$ ratio in the KF solution (0.65) approached a value similar to that of the fully stabilized α-helix (approximately 0.86).[31] Moreover, the change in α-helical content was negligible when the temperature was increased from 4 to 25 °C in the KF solution, indicating stable structure formation.

Surprisingly, the $[\theta]_{222}/[\theta]_{208}$ ratio even increased to 0.74 at a highly elevated temperature (74 °C) (Figure 4b). Therefore, we further scrutinized the effect of temperature on helicity. As shown in Figure 4c, a temperature ramp experiment revealed that the $[\theta]_{222}/[\theta]_{208}$ ratio did gradually increase as the temperature was raised, and the process was reversible. The occurrence of hysteresis during the forward and reverse scans is likely associated with the kinetic effect on self-assembly. Plotting $[\theta]_{222}$ as a function of temperature showed that decrease in the ellipticity value at 222 nm was very small as the temperature increased (Figure 4d).

Many thermostable proteins show a drastic increase in the number of hydrophobic residues in the core of the protein or at a subunit interface. Because hydrophobic effects increase with temperature, the increased hydrophobic interaction at elevated temperatures is believed to be a critical factor for the structural stabilization in thermostable proteins.[14] In addition, the oligomerization of monomeric subunits has been shown to

dx.doi.org/10.1021/bm400233x | Biomacromolecules 2013, 14, 1594−1599

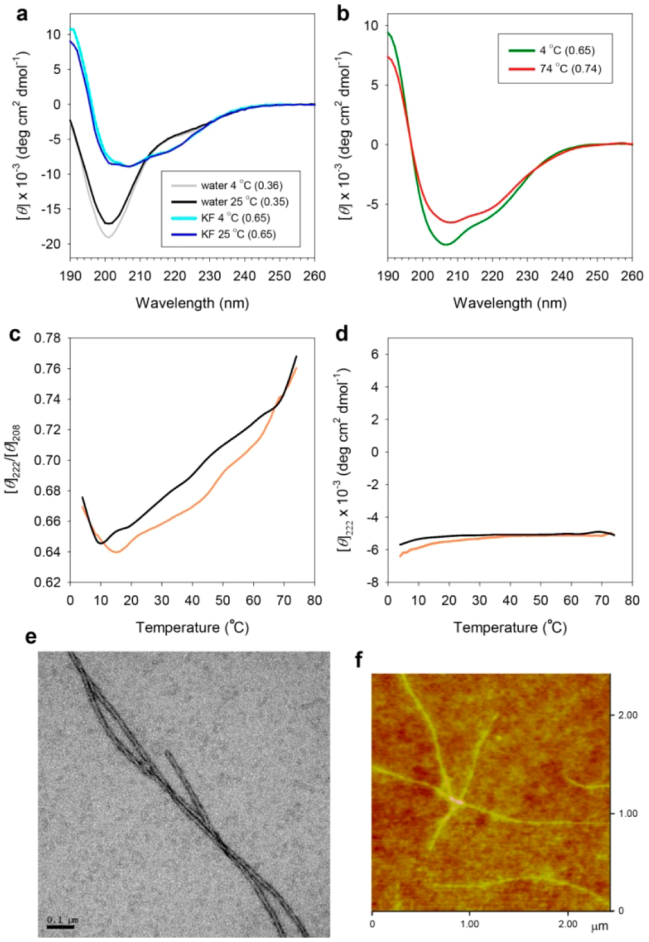

Figure 4. Self-assembled nanofiber of the SA-Rev_{12-64} PA with highly stable α-helices. (a) CD spectra in water or 60 mM KF. [peptide] = 15 μM. (b) CD spectra of the peptide in 60 mM KF at different temperatures. [peptide] = 15 μM. Values in parentheses represent the $[\theta]_{222}/[\theta]_{208}$ ratios. (c, d) Temperature ramp experiments (15 μM peptide). Forward scan (orange); reverse scan (black). (e) Negative-stain TEM micrograph. Bar = 0.1 μm. (f) AFM image.

improve the stability of many thermophilic proteins.[13] Therefore, the combined effect of strongly hydrophobic core formation and self-assembly is likely responsible for the observed high thermostability in SA-Rev_{12-64} PA assembly. Taken together, these results indicate that SA-Rev_{12-64} PAs assemble into extremely thermostable helical hairpin structures and the effect of stearic acid conjugation is very significant.

The nanostructure morphology of the SA-Rev_{12-64} PA aggregates was visualized by transmission electron microscopy (TEM). The results showed that the predominant forms of the self-assembled nanostructures were discrete nanofibers (Figure 4e). The thickness of the nanofiber was 14 ± 1 nm. Investigation by atomic force microscopy (AFM) further confirmed the formation of nanofibers (Figure 4f). Rev helical hairpins are known to initially form a V-shaped dimer via tail-to-tail interactions; this dimer then further oligomerizes using two hydrophobic head faces in the dimer. Combining all of the results obtained from this study and the previous structural data available in the literature,[17−19,32] we modeled the fibrous nanostructures of the SA-Rev_{12-64} PAs (Figure 1d). The SA-Rev_{12-64} PAs first dimerize into a V-shaped topology through hydrophobic interactions between tail faces and between stearate chains, followed by multimerization through hydrophobic interactions between head faces and between stearate chains. The overall processes stabilize the helical hairpin structures. The stearate chains constitute the internal part of the nanofiber, forming a stable hydrophobic core.

CONCLUSIONS

We have devised a novel bioinspired self-assembly strategy to construct nanostructures with multiple and highly thermostable α-helical structures. The Rev peptide and stearic acid conjugates can be viewed as amphiphiles with the Rev ARM and proline-rich loop as the hydrophilic part, and the oligomerization domain and alkyl chain as the hydrophobic part (Figures 1b,c and S7). Nanostructures could not be obtained without stearate conjugation; therefore, the hydrophobic modification of the Rev peptide was crucial for forming the self-assembled nanostructures and the subsequent helix stabilization. Previously, self-assembly mediated helix stabilization was achieved by constraining the α-helical segment within a macrocyclic scaffold.[11] However, the stabilization effect could not be obtained when the self-assembling peptides had linear structures.[33] The overall configuration of the peptide building blocks used in this study is linear; however, the Rev ARM α-helical domain was efficiently constrained because the N- and C-terminal ends of the Rev_{12-64} PA could be firmly connected by strong noncovalent hydrophobic interactions. This phenomenon might be referred to as a "pseudo-cyclization effect." Because cyclization reactions for large molecules are often difficult to perform, the noncovalent method described in this report provides a suitable alternative to using covalently connected macrocycles for helix stabilization.

ASSOCIATED CONTENT

Supporting Information

Peptide chemical structures, MALDI-TOF MS spectra, additional structural information, FP spectra, solubility data, and additional TEM data. This material is available free of charge via the Internet at http://pubs.acs.org.

AUTHOR INFORMATION

Corresponding Author

*E-mail: yblim@yonsei.ac.kr.

Notes

The authors declare no competing financial interest.

ACKNOWLEDGMENTS

This work was supported by grants from the National Research Foundation (NRF) of Korea (Basic Science Research Program, 2012R1A1A2006453; Translational Research Center for Protein Function Control, 2012-0000888) and from the Seoul R&BD program (ST110029).

REFERENCES

(1) Pace, C. N.; Scholtz, J. M. *Biophys. J.* **1998**, *75*, 422−427.
(2) Rizo, J.; Gierasch, L. M. *Annu. Rev. Biochem.* **1992**, *61*, 387−418.
(3) Sia, S. K.; Carr, P. A.; Cochran, A. G.; Malashkevich, V. N.; Kim, P. S. *Proc. Natl. Acad. Sci. U.S.A.* **2002**, *99*, 14664−14669.
(4) Walensky, L. D.; Kung, A. L.; Escher, I.; Malia, T. J.; Barbuto, S.; Wright, R. D.; Wagner, G.; Verdine, G. L.; Korsmeyer, S. J. *Science* **2004**, *305*, 1466−1470.
(5) Zhang, F.; Sadovski, O.; Xin, S. J.; Woolley, G. A. *J. Am. Chem. Soc.* **2007**, *129*, 14154−14155.
(6) Ruan, F. Q.; Chen, Y. Q.; Hopkins, P. B. *J. Am. Chem. Soc.* **1990**, *112*, 9403−9404.

(7) Marqusee, S.; Baldwin, R. L. *Proc. Natl. Acad. Sci. U.S.A.* **1987**, *84*, 8898−8902.
(8) Johnson, L. M.; Mortenson, D. E.; Yun, H. G.; Horne, W. S.; Ketas, T. J.; Lu, M.; Moore, J. P.; Gellman, S. H. *J. Am. Chem. Soc.* **2012**, *134*, 7317−7320.
(9) Patgiri, A.; Joy, S. T.; Arora, P. S. *J. Am. Chem. Soc.* **2012**, *134*, 11495−11502.
(10) Doig, A. J.; Chakrabartty, A.; Klingler, T. M.; Baldwin, R. L. *Biochemistry* **1994**, *33*, 3396−3403.
(11) Lim, Y. B.; Moon, K. S.; Lee, M. *Angew. Chem., Int. Ed.* **2009**, *48*, 1601−1605.
(12) Choi, S. J.; Jeong, W. J.; Kim, T. H.; Lim, Y. B. *Soft Matter* **2011**, *7*, 1675−1677.
(13) Forns, P.; Lauer-Fields, J. L.; Gao, S.; Fields, G. B. *Biopolymers* **2000**, *54*, 531−546.
(14) Sim, S.; Kim, Y.; Kim, T.; Lim, S.; Lee, M. *J. Am. Chem. Soc.* **2012**, *134*, 20270−20272.
(15) Pollard, V. W.; Malim, M. H. *Annu. Rev. Microbiol.* **1998**, *52*, 491−532.
(16) Battiste, J. L.; Mao, H.; Rao, N. S.; Tan, R.; Muhandiram, D. R.; Kay, L. E.; Frankel, A. D.; Williamson, J. R. *Science* **1996**, *273*, 1547−1551.
(17) Jain, C.; Belasco, J. G. *Mol. Cell* **2001**, *7*, 603−614.
(18) Daugherty, M. D.; Liu, B.; Frankel, A. D. *Nat. Struct. Mol. Biol.* **2010**, *17*, 1337−1342.
(19) DiMattia, M. A.; Watts, N. R.; Stahl, S. J.; Rader, C.; Wingfield, P. T.; Stuart, D. I.; Steven, A. C.; Grimes, J. M. *Proc. Natl. Acad. Sci. U.S.A.* **2010**, *107*, 5810−5814.
(20) Tan, R.; Chen, L.; Buettner, J. A.; Hudson, D.; Frankel, A. D. *Cell* **1993**, *73*, 1031−1040.
(21) Wang, D.; Chen, K.; Kulp Iii, J. L.; Arora, P. S. *J. Am. Chem. Soc.* **2006**, *128*, 9248−9256.
(22) Ghosh, T.; Kalra, A.; Garde, S. *J. Phys. Chem. B* **2005**, *109*, 642−651.
(23) Lim, Y. B.; Lee, E.; Lee, M. *Angew. Chem., Int. Ed.* **2007**, *46*, 3475−3478.
(24) Marqusee, S.; Robbins, V. H.; Baldwin, R. L. *Proc. Natl. Acad. Sci. U.S.A.* **1989**, *86*, 5286−5290.
(25) Hartgerink, J. D.; Beniash, E.; Stupp, S. I. *Science* **2001**, *294*, 1684−1688.
(26) McGregor, C. L.; Chen, L.; Pomroy, N. C.; Hwang, P.; Go, S.; Chakrabartty, A.; Prive, G. G. *Nat. Biotechnol.* **2003**, *21*, 171−176.
(27) Webber, M. J.; Tongers, J.; Newcomb, C. J.; Marquardt, K. T.; Bauersachs, J.; Losordo, D. W.; Stupp, S. I. *Proc. Natl. Acad. Sci. U.S.A.* **2011**, *108*, 13438−13443.
(28) Lim, Y. B.; Lee, E.; Lee, M. *Angew. Chem., Int. Ed.* **2007**, *46*, 9011−9014.
(29) Roccatano, D.; Colombo, G.; Fioroni, M.; Mark, A. E. *Proc. Natl. Acad. Sci. U.S.A.* **2002**, *99*, 12179−12184.
(30) Lynn, J.; Fasman, G. D. *Biopolymers* **1968**, *6*, 159−163.
(31) McNamara, C.; Zinkernagel, A. S.; Macheboeuf, P.; Cunningham, M. W.; Nizet, V.; Ghosh, P. *Science* **2008**, *319*, 1405−1408.
(32) Watts, N. R.; Misra, M.; Wingfield, P. T.; Stahl, S. J.; Cheng, N.; Trus, B. L.; Steven, A. C.; Williams, R. W. *J. Struct. Biol.* **1998**, *121*, 41−52.
(33) Han, S.; Kim, D.; Han, S. H.; Kim, N. H.; Kim, S. H.; Lim, Y. B. *J. Am. Chem. Soc.* **2012**, *134*, 16047−16053.